

# External strengthening of unreinforced masonry walls with polymers reinforced with carbon fiber

## Reforzamiento externo de muros de mampostería no reforzada mediante polímeros reforzados con fibra de carbono

Camilo Vega<sup>1</sup>, Nancy Torres<sup>2</sup>

### ABSTRACT

In many countries, buildings are usually made of unreinforced clay masonry walls, especially in Colombia. These constructions have low resistance and ductility, and are very vulnerable to seismic events, due to their low capacity of energy dissipation. This paper reports the results obtained from a research project that evaluates the behavior of reinforced masonry walls under lateral loads. The reinforcement was made using Carbon Fiber Reinforced Polymers (CFRP). In the test program, eight (8) clay masonry walls were built using hollow brick. Four (4) of them were 1,23 m long and 1,90 m high and the remaining four (4) were 2,47 m long and 1,90 m high. Four (4) walls were tested with a static lateral load and four (4) with a cyclic lateral load in its plane. Results revealed that the presence of the reinforcement material significantly increased the ultimate load and deformation capacity, provided that the material has a suitable anchoring system.

**Keywords:** Unreinforced masonry, fiber reinforced polymers, seismic retrofitting, lateral loads.

### RESUMEN

La construcción de viviendas con muros de mampostería en arcilla no reforzada es tradicional en muchos países, en especial en Colombia. Debido a su baja resistencia y ductilidad, estas edificaciones son muy vulnerables a eventos sísmicos como consecuencia de su poca capacidad de disipación de energía, lo que genera fallas que llevan incluso al colapso total. Este artículo expone los resultados de un proyecto de investigación donde se evaluó el comportamiento ante cargas laterales en muros de mampostería no estructural, reforzados mediante polímeros reforzados con fibra de carbono (CFRP). En el programa experimental, se construyeron ocho (8) muros de mampostería de arcilla, utilizando bloque de perforación horizontal. Cuatro (4) de ellos tenían dimensiones de 1,23 m de largo por 1,90 m de alto y los cuatro (4) restantes de 2,47 m de largo por 1,90 m de alto. Cuatro (4) muros se probaron ante carga lateral estática y cuatro (4) ante carga lateral cíclica en su plano. Los resultados muestran que el material de refuerzo mejoró significativamente la capacidad de carga y deformación última de los muros, siempre y cuando se tenga un adecuado sistema de anclaje.

**Palabras clave:** Mampostería no reforzada, polímeros reforzados con fibra, reforzamiento sísmico, cargas laterales.

**Received:** June 27th 2018

**Accepted:** December 5th 2018

### Introduction

Buildings made of unreinforced masonry walls are structures characterized by their inadequate behavior against earthquakes, due to their low ductility and low energy dissipation capability. Consequently, these structures are very vulnerable to these phenomena and can suffer sudden failures that could lead them even to a total collapse. This has been observed in previous earthquakes, such as those of Popayán, Colombia in 1983 (Ingeominas, 1986), Northridge, U.S.A. in 1994 (Klingner, 2006), Eje Cafetero, Colombia in 1999 (Ingeominas, 1999), Tecomán, Mexico in 2003 (Klingner, 2006), and the central coastal region of Chile in 2010 (FOPAE, 2010), among others.

Fiber Reinforced Polymers (FRP) are compounds known as an alternative for the reinforcement of masonry structures. They are characterized for being lightweight and non-corrosive, and for having a high tensile strength, and a high elasticity modulus. These polymers are also commercially

available in various types, which include sheets, fabric, and reinforcement bars (ACI 440-7R, 2010).

Several researches have demonstrated that FRP systems are effective in increasing the shear and flexural strength of masonry walls subjected to in-plane loads. The structural

<sup>1</sup> Civil Engineer, M.Sc. in Civil Engineering, Escuela Colombiana de Ingeniería Julio Garavito, Colombia. Affiliation: Instructor Professor, Escuela Colombiana de Ingeniería Julio Garavito. E-mail: [camilo.vega@escuelaing.edu.co](mailto:camilo.vega@escuelaing.edu.co).

<sup>2</sup> Civil Engineer, Universidad Francisco de Paula Santander, Colombia. Ph.D. Materials Science and Technology, Universidad Nacional de Colombia, Colombia. Affiliation: Associate Professor, Escuela Colombiana de Ingeniería Julio Garavito, Colombia. E-mail: [nancy.torres@escuelaing.edu.co](mailto:nancy.torres@escuelaing.edu.co).

**How to cite:** Vega, C., Torres, N. (2018). External strengthening of unreinforced masonry walls with polymers reinforced with carbon fiber. *Ingeniería e Investigación*, 38(3),15-23. DOI: [10.15446/ing.investig.v38n3.73151](https://doi.org/10.15446/ing.investig.v38n3.73151)



Attribution 4.0 International (CC BY 4.0) Share - Adapt

performance of the FRP-strengthened masonry wall depends on the configuration of the reinforcement (Valluzzi *et al.*, 2002; Elgawady *et al.*, 2006; Galati *et al.*, 2006; Gabor *et al.*, 2006; Tumialan *et al.*, 2009; Capozzuca, 2011; Santa-Maria & Alcaino, 2011; Triantafillou *et al.*, 2011; Mosallam & Banerjee, 2011; Luccioni & Rougier, 2011; Kalali & Kabir, 2012; Lopez, 2012; Arifuzzaman & Saatcioglu, 2012; Lignola *et al.*, 2012; Lunn *et al.*, 2013; Rahman & Ueda, 2016).

In recent years, the external reinforcement of masonry walls with FRP strips has become more common in Colombia. However, the current construction code (NSR-10) does not consider these materials as a reinforcement alternative and studies lack on this subject. Thus, this research seeks to be a contribution to the behavior of these emerging materials, so that they can be considered as an external reinforcement for clay walls. This study also contemplates the considerations and requirements that must be taken into account for an adequate load transfer to the floor and the foundation.

## Experimental program

The wall specimens for this research included slender and squat walls subjected to in-plane loads. Aspect ratios are typically  $H/L > 1$  for slender walls and  $H/L < 1$  for squat walls ( $H$  is the height and  $L$  is the length).

### Description of the Wall Specimens

Eight masonry walls were constructed for this experimental program. Aiming to study the shear strength in the walls, two slenderness ratios were used: one of 1,54 (flexure) and another of 0,77 (shear). Four walls of 1,23 m length and 1,90 m height were built with the first relation. The remaining four were 2,47 m length and 1,90 m height. The specimens were placed over a foundation beam with a cross section of 0,25x0,30 m and a length of 1,73 m for the slender walls, and 2,97 m for the squat walls. The base beams were reinforced with two #5 diameter steel bars, top and bottom, and #4 diameter closed steel stirrups with 150 mm spacing between them. The base beams were designed to resist expected bending moments and shear forces due to the anchor points at the wall base resisting the in-plane loads. On the top side of the walls, another beam was built as boundary element. Its cross-section dimensions were 0,15x0,15 m and its length was determined by the wall. These beams were reinforced with minimum steel reinforcement. Their function was to cap the top of the wall in order to place the hydraulic actuator.

### Materials

The test specimens were built with hollow clay masonry units, commonly known in Colombia as block No. 5, of nominal dimensions 0,30x0,20x0,12 m (Fig.1). Masonry prisms were made to determine their compressive strength. Table 1 summarizes the engineering properties of the

masonry material, as well as those of concrete, steel and FRP system, as reported by the manufacturer. It also includes the properties of the epoxy used to anchor the walls.

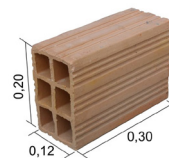


**Figure 1.** Dimensions of block No.5 (m).

**Source:** Authors

### Wall strengthening schemes

FRP systems are usually installed to increase the strength of URM walls. The basic wall strengthening scheme encompassed: 1) the Carbon Fiber Reinforced Polymer (CFRP) strengthening of the masonry walls to resist stresses due to the in-plane loads, and 2) the anchorage of the wall to the concrete beams, to provide a load path for the in-plane loads, so that the strengthened wall could function effectively as a lateral-load resisting element. The wall specimens were strengthened with CFRP strips, which were installed using the manual lay-up technique. This reinforcement was fitted on just one face of the wall and anchored on its opposite side. There were two reinforcement layouts: grid and diagonal. The grid layout involved the installation of five horizontal CFRP strips of 0,10 m wide, spaced every 0,40 m; and two vertical ones at each end of the wall, of 0,10 m wide for slender walls, and 0,15 m for squat walls (Fig.2a). The diagonal layout involved the installation of four diagonal CFRP strips of 0,10 m wide, oriented at approximately 45° degrees to the horizontal side (Fig. 2b). The designs of the FRP reinforcements for the sample specimens were based on the guidelines established in the ACI 440.7R-10 document. The design philosophy is based on limit state design principles.

**Table 1.** Material properties

Material	Property	
Masonry	Compressive strength of masonry unit, $f'_{cu}$ , (NTC 4017):	9,8 MPa
	Compressive strength of masonry, $f'_m$ (ASTM C1314 / NTC 3495):	5,3 MPa
	Compressive strength of mortar, $f'_{cp}$ (ASTM C270 / NTC 220):	20 MPa
Reinforced Concrete	Compressive strength of concrete, $f'_c$ (ASTM C39 / NTC 673):	28 MPa
	Steel yield strength, $f_y$ (ASTM A615 / NTC 2289):	420 MPa
CFRP System (*)	Tensile strength (ASTM D7205):	651 MPa
	Strain at ultimate (ASTM D7205):	1,55 %
	Modulus of elasticity (ASTM D7205):	62,4 GPa
Epoxy (*)	Strip thickness (ASTM D7205):	1,016 mm
	Tensile strength (ASTM D638):	29,7 MPa
	Elongation at break (ASTM D638):	1,3%

(\*) Values reported by the manufacturer

**Source:** Authors

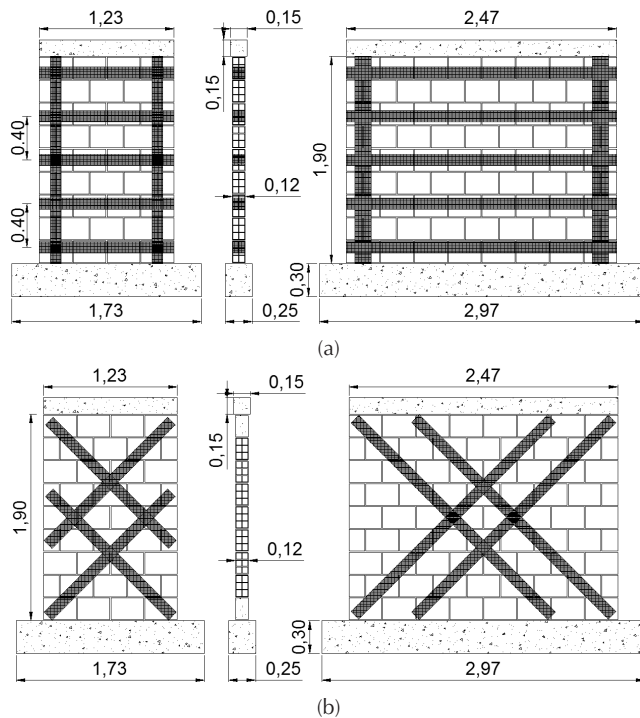


**Figure 2.** Dimensions (m) and reinforcement: (a) Slender and squat grid-walls; (b) Slender and squat diagonal-walls.

**Source:** Authors

In order to completely connect the wall to its foundation, guaranteeing its behavior as a shear wall, the anchorage system for the strengthened walls involved the removal of selected masonry units at the edges of their bottom row. From each edge, one unit and two and a half units were removed in the slender and squat walls, respectively. As replacement of these units, concrete blocks were built. Two #4 diameter epoxy-anchor hooked steel bars were embedded 150 mm into the base beam for building a repair grout solid block. This procedure was done in two phases, leaving a gap at the bottom for wrapping the CFRP strip around the grout block and through the gap. Before wrapping the polymer, the corners of the grout blocks were rounded to a 50 mm radius. Finally, the gap was filled with an additional grout. Figure 3 shows the installation of the anchorage system for the squat walls. This anchor system was employed for strengthened specimens only. The horizontal strips were anchored on the opposite side of the wall.

Table 2 summarizes the walls tested as part of this research. UR-SL and UR-SQ are the slender and squat unreinforced masonry walls (control specimens), respectively. The strengthened walls are labeled based on the strengthening layout, 'G' (Grid) or 'D' (Diagonal). Depending on the aspect ratio, the walls are classified into SL for slender walls or SQ for squat walls. Finally, 'M' indicates a monotonic test and 'C' indicates a cyclic one. For example, the specimen G-SQ-C is a squat wall strengthened in grid layout, with cyclic test.

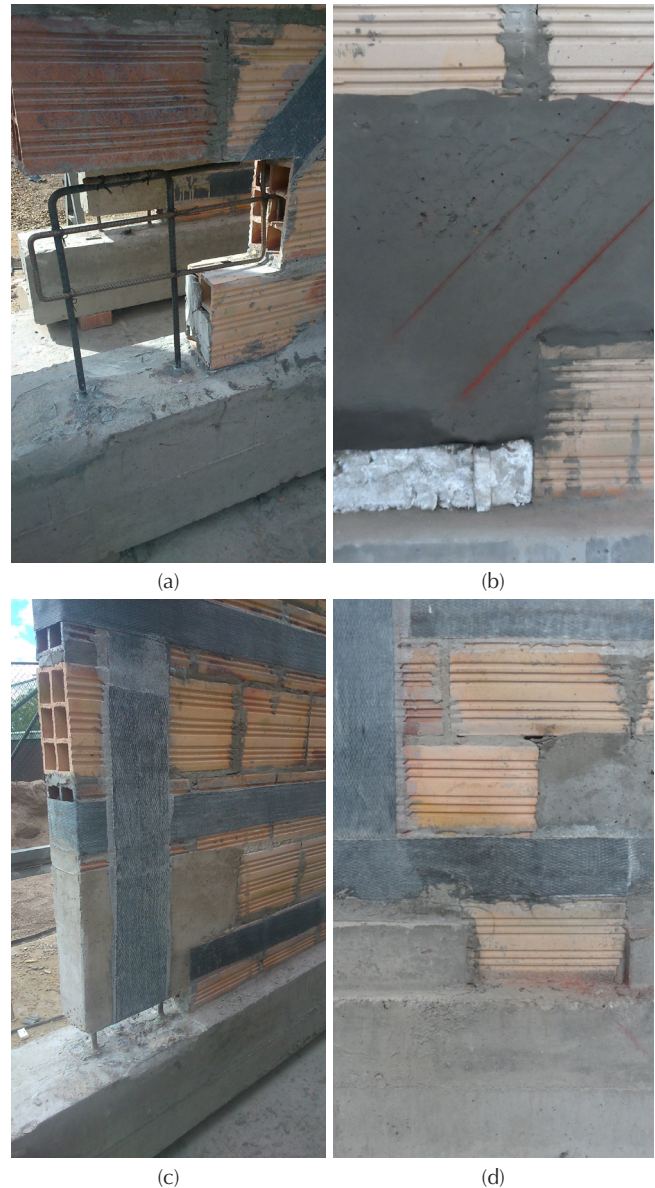


**Figure 3.** Construction process of the anchorage system: (a) removed masonry units and hooked steel bars; (b) placed grout block with bottom gap; (c) installed FRP strip wrapped around grout block; and (d) additional grout filling the gap.

**Source:** Authors

**Table 2.** Summary of walls tested

No.	Type Test	Aspect ratio	CFRP Layout	Specimen ID
1	Monotonic	Slender	None	UR-SL
2		Squat	None	UR-SQ
3		Slender	G	G-SL-M
4		Squat	D	D-SQ-M
5	Cyclic	Slender	G	G-SL-C
6		Squat	G	G-SQ-C
7		Slender	D	D-SL-C
8		Squat	D	D-SQ-C

**Source:** Authors

## Testing of walls

The testing program consisted of two phases. The first phase involved monotonic loading of wall specimens. The second phase involved cyclic loading of wall specimens. Both phases and their objectives are described below.

- **Monotonic loading:** The primary objective of this phase was to evaluate the anchorage system. This phase involved testing of four walls under monotonic in-plane loads, including two unreinforced masonry walls used as control specimens. The monotonic in-plane load was applied at a load rate of 0,22 kN/s, until reaching failure of the anchorage system.
- **Cyclic loading:** The objective of this series was the evaluation of the two strengthening layouts working in conjunction with the anchorage system. This series involved the testing of four walls under in-plane cyclic lateral load, following a displacement-controlled method as specified by the FEMA 461. The loading sequence consisted in repeated cycles of step-wise increasing deformation amplitudes. Two cycles for each amplitude were done. Figure 4 shows the loading protocol. The cyclic load was applied at a frequency of 0,15 Hz.

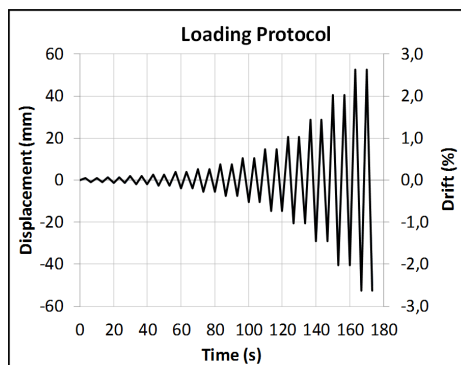


Figure 4. Loading protocol.  
Source: Authors

The walls were tested at the Structural Laboratory of the Escuela Colombiana de Ingeniería Julio Garavito in Bogotá, Colombia. The walls were tested within a steel structure used as reaction frame. The reaction frame is a permanent steel structure anchored to the structural floor of the laboratory and designed to resist in-plane loads of up to 300 kN. The reaction frame consists of two built-up steel columns in the sides and two built-up steel beams in the top and bottom. For monotonic tests, the in-plane loads were generated by a hydraulic jack that had a capacity of 250 kN. During the test, the force was measured with a load cell of 50 kN of capacity, and sensitivity of 10 N. For the cyclic tests, in-plane loads were generated by a pseudo-dynamic hydraulic actuator mounted on a column of the reaction frame and connected to the top of the test wall.

To prevent rocking, the concrete base beam was connected to the bottom frame beam using structural steel shapes

and high-strength steel rods. To prevent sliding, structural steel struts were installed between the beam ends of the concrete base and the frame columns. The test configuration without load applied at the top of the wall provides the most adverse condition for the anchorage at the wall base. Besides, walls built with blocks of clay with horizontal perforations are commonly used in one- or two-story buildings, where the axial load is low. Three Linear Variable Differential Transducers (LVDTs) were used to monitor the wall displacements at the top and bottom.

Figure 5 shows an overall view of the test setup and illustrates the location of the instrumentation. The loading process was suspended once the failure of the wall was reached, which corresponds to a drift of 2,5%.

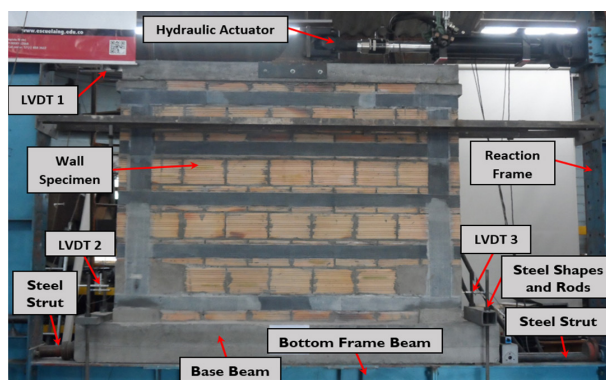
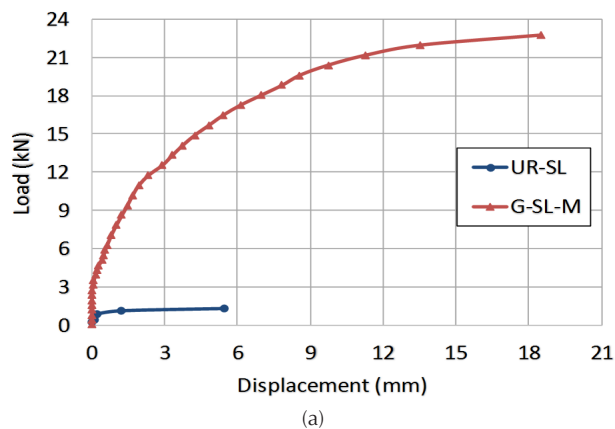


Figure 5. Overall view of the test setup.  
Source: Authors

## Experimental results

### Monotonic in-plane loading

Table 3 presents the maximum load that each wall resisted in the monotonic tests, while Figure 6 presents the load resisted versus the lateral displacement registered.



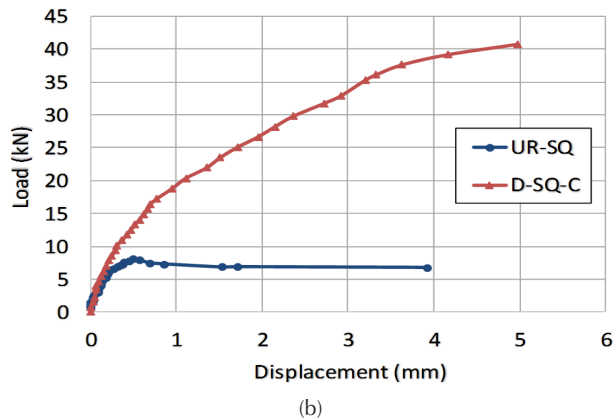


**Figure 6.** Load vs. Lateral Displacement: (a) Slender walls; (b) Squat walls.  
Source: Authors

In the squat wall with diagonal reinforcement, there is a significant increase in the resistance to lateral loads. This wall reached resistances 5 times greater than those of unreinforced walls. Regarding the slender wall with grid reinforcement, performance is even greater, as it achieved resistance 18 times greater than the one of the unreinforced wall.

**Table 3.** Experimental results

No	Test Type	Specimen ID	V(kN)	Mode of Failure
1	Monotonic	UR-SL	1,3	Flexure at wall base
2		UR-SQ	8,2	Flexure at wall base
3		G-SL-M	23,4	Flexure near wall base
4		D-SQ-M	40,9	Flexure near wall base with rupture of FRP at grout block
5	Cyclical	G-SL-C	24,4	Flexure near wall base and adherence loss of the CFRP
6		G-SQ-C	66,6	Flexure near wall base and adherence loss of the CFRP
7		D-SL-C	16,5	Flexure near wall base with rupture of FRP at grout block
8		D-SQ-C	56,7	Flexure near wall base with rupture of FRP at grout block

Source: Authors

### Failure modes

The test results of the control walls showed that the flexural failure occurred at the base of the walls. This type of failure was expected given that the walls were essentially cantilever elements. In cantilever masonry walls, such as those tested in this research, the initial crack typically appears at the base of the tested wall. Failure modes of the two URM control walls (UR-SL and UR-SQ) initiated with a single flexural horizontal crack along the mortar joint above the first row of masonry units (Fig.7). No toe crushing or diagonal cracking was evidenced. The flexural failure occurred at loads of 1,3 kN and 8,2 kN for UR-SL and UR-SQ, respectively.



**Figure 7.** Failure mode of the URM walls.  
Source: Authors

Diagonally reinforced walls failed due to the rupture of the CFRP wrapped around the grout block at the base. Moreover, debonding and delamination of the reinforcement from the wall was observed, which generated tensile-related failures and breaking of some masonry units (Fig.8a). Although the squat specimens showed a principal staircase-shaped crack, it initiated at the medium part of the wall and extended to its base (Fig.8b). Once again, the rupture of the fiber in the anchoring region indicates that the main failure was flexural.

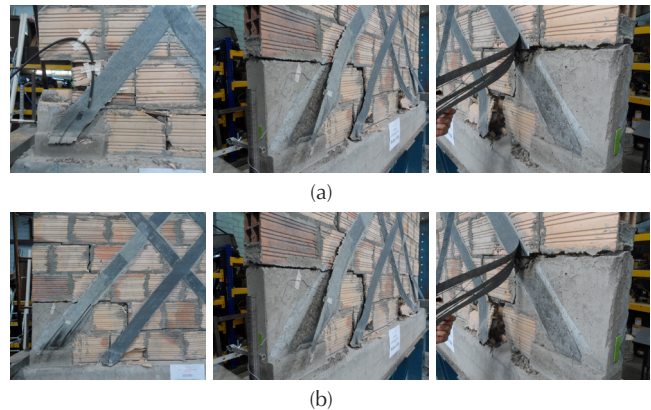


**Figure 8.** Failure mode of the diagonally reinforced walls: (a) Slender walls; (b) Squat walls.  
Source: Authors

Grid-reinforced specimens presented flexural failure as well. The breaking of masonry units along the principal cracks was very common, due to the compressive stress. These cracks were located within the first row of mortar, and between the wall and the concrete blocks. This failure generated wall displacement, relative to one of the anchoring blocks. This was observed in the squat specimen, which decreased its loading capacity (Fig.9b). Otherwise, in the slender wall, a failure was produced at the joint of the grout from the anchoring system, while a series of tensile related fissures appeared in some units at the base of the wall (Fig.9a). Due to this behavior, the CFRP could not work at its maximum capacity, and only showed a small failure related to adherence in the grout block region (Fig.9b).

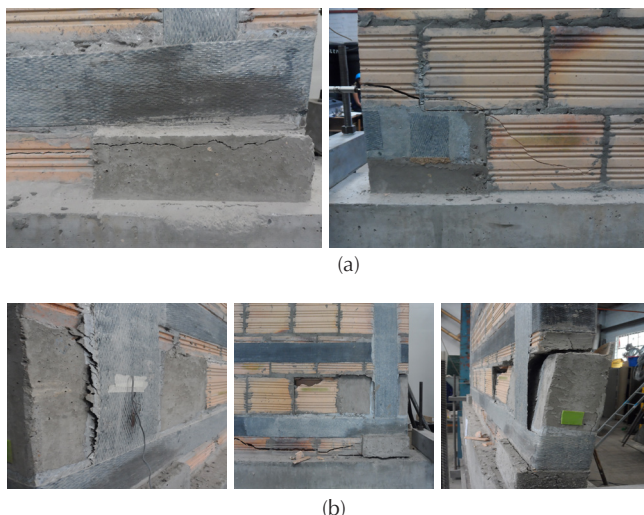


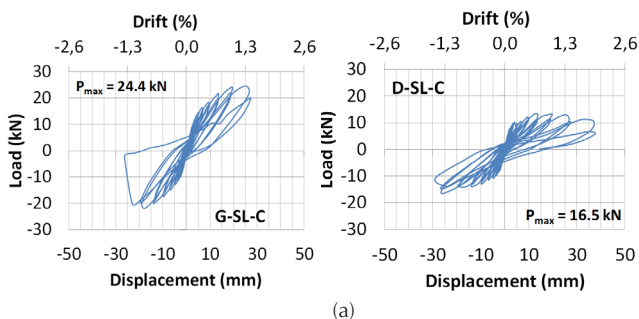
**Figure 9.** Failure mode of the grid reinforced walls: (a) Slender walls; (b) Squat walls.  
**Source:** Authors

*Cyclic in-plane loading*

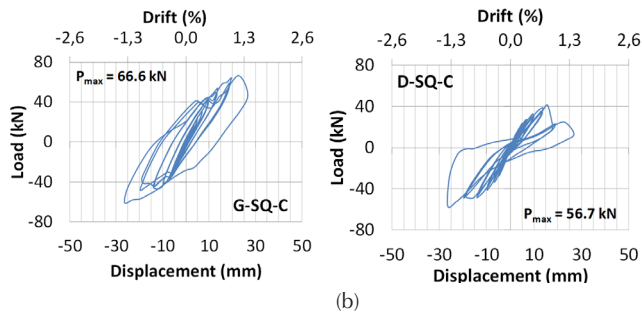
Table 3 shows the maximum loading capacity results for each wall during the cyclic tests. The grid reinforcement presents higher values than the specimens with a diagonal layout reinforcement. It is important to highlight that the fiber area relationship between the grid and diagonal layouts was of 1.5. Moreover, in comparison with the unreinforced slender walls, the ones with diagonal reinforcement presented resistance 12,7 times greater, and those with grid configuration, 18,8 times greater. Additionally, for the squat walls, these values were 6,9 and 8,1 times greater, with diagonal and grid layouts, respectively. This shows that the reinforcement material improves significantly the resistance and performance of these elements when subjected to the studied loads.

*Hysteretic response*

The hysteretic responses of the walls under cyclic loading are shown in Figure 10. The envelopes of the curves for slender and squat walls are shown in Figure 11.



(a)



(b)

**Figure 10.** Hysteretic responses of the walls: (a) Slender walls; (b) Squat walls.  
**Source:** Authors

These envelopes show that slender and squat walls have a linear elastic behavior, until the drift reaches approximately 0,3%; except specimens G-SQ-C, which reached a value of 0,5%. From these values, the performance of the walls can be inelastic, with loading and unloading cycles that decrease the elements rigidity until the displacement reaches 2,0% in slender walls, and 1,3% in squat walls. Finally, the increase of important fissures and the degradation of rigidity decrease the loading capacity of the element.

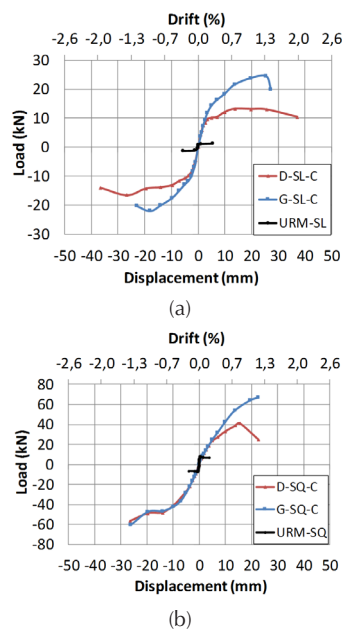


**Figure 11.** Envelopes of the hysteresis curves: (a) Slender walls; (b) Squat walls.  
**Source:** Authors

*Lateral stiffness*

The NSR-10 prescribes an allowable story drift of 0,5% for masonry cantilever shear walls, such as those tested in this research. Even if the failure mode is mainly flexural (like the foregoing), the story drift can reach 1,0%. Figure 12 illustrates the degradation of the lateral stiffness (secant stiffness) of the slender and squat walls, measured as the lateral load divided into the corresponding displacement in

every cycle of the tests. Table 4 summarizes the degradation of lateral stiffness for allowable drifts of 0,5% and 1,0%. As the loading and unloading cycles advance, the decrease of this property with a drift of 0,5% is low. In general terms, the walls with the “G” layout show less degradation of the lateral stiffness when compared to those strengthened with the “D” layout.

After the initial cracking of the slender walls, the ones strengthened with the ‘G’ layout showed stiffness degradation (measured relative to the initial lateral stiffness,  $K_0$ ) around 4% for an allowable drift of 0,5% and 23% for an allowable drift of 1,0%. The stiffness degradation was greater in the walls strengthened with the ‘D’ Layout, as it was of about 10% for an allowable drift of 0,5 % and around 41% for an allowable drift of 1,0%.

After the initial cracking of the squat walls, the ones strengthened with the ‘G’ Layout, showed stiffness degradation around 6% for an allowable drift of 0,5% and about 14% for an allowable drift of 1,0%. The degradation of stiffness was larger in the walls strengthened with the ‘D’ Layout: approximately 9% for an allowable drift of 0,5 % and around 25% for an allowable drift of 1,0%.

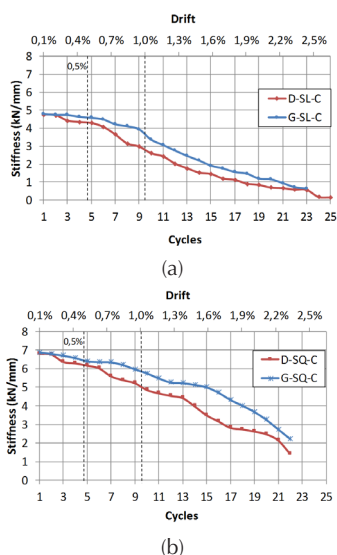


**Figure 12.** Degradation of the lateral stiffness: (a) Slender walls; (b) Squat walls.  
**Source:** Authors

**Table 4.** Lateral stiffness degradation

Specimen ID	$K_0$ (kN/mm)	At 0,5%		At 1,0%	
		K (kN/mm)	% Degradation	K (kN/mm)	% Degradation
G-SL-C	4,80	4,60	4	3,70	23
D-SL-C	4,76	4,30	10	2,80	41
G-SQ-C	6,88	6,48	6	5,90	14
D-SQ-C	6,81	6,23	9	5,10	25

**Source:** Authors

### Ductility

In order to calculate the ductility and energy dissipation capacity in the inelastic range of the walls, the methodology described by Paulay & Priestley (1992) was used. Unreinforced masonry structures typically have short periods. For structures with short periods, ductility can be measured using the equal-energy principle. In this approach, the displacement ductility factor ( $\mu$ ) is estimated by equating the area under the inelastic force-deflection curve and the area under the elastic relationship, with equal initial stiffness, as shown in Figure 13. From this figure, the relationship between the displacement ductility factor and the force reduction factor ( $R$ ) can be expressed as. From this equation,  $R$  for short-period structures can be expressed as. The displacement ductility was computed as, where  $\Delta_m$  is the maximum displacement and  $\Delta_y$  is the displacement at yielding. The slender walls show higher ductility values than the squat walls, in approximately 1,5 times, which was expected since slender walls are less stiff. Table 5 summarizes the displacement ductility factors ( $\mu$ ) and the force reduction factors ( $R$ ) calculated for the slender and squat walls. The  $R$  factors obtained for the slender and squat walls are approximately 3,6 and 2,8, respectively.

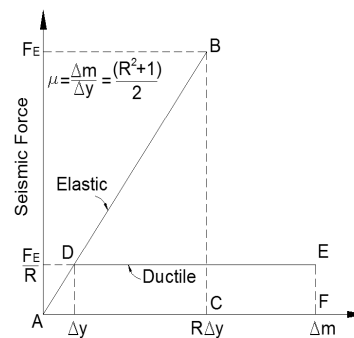


**Figure 13.** Relationship between ductility and force reduction factors -  $R$ .

**Source:** Paulay & Priestley, 1992, p.77

**Table 5.** Displacement ductility factors and force reduction factors

Specimen ID	$\Delta_y$ (mm)	$\Delta_{max}$ (mm)	$\mu$	$R$
G-SL-C	3,75	25,56	6,82	3,55
D-SL-C	3,80	26,28	6,92	3,58
G-SQ-C	6,10	26,29	4,31	2,76
D-SQ-C	5,80	26,35	4,54	2,84

**Source:** Authors

The ASCE 7 and NSR-10 assign the following values of  $R$  for different types of shear walls:

- Ordinary plain masonry shear walls (URM):  $R = 1,5$ ;  $R = 1,0$
- Ordinary reinforced masonry shear walls:  $R = 2,0$ ;  $R = 2,0$
- Intermediate reinforced masonry shear walls:  $R = 3,5$ ;  $R = 2,5$
- Special reinforced masonry shear walls:  $R = 5,5$ ;  $R = 3,5$

A preliminary comparison and the ASCE 7 and NSR-10 values reveals a substantial increase of R when compared to ordinary plain masonry shear walls (URM shear walls). The squat walls reflect better the geometry of a typical shear wall. In that case, the calculated R of 2.8 exceeds the value of 2,0 specified by the ASCE 7 and NSR-10 for ordinary reinforced masonry shear walls.

## Conclusions

The use of FRP as reinforcement material decreased fragile failure on the walls. When compared with control walls, the greatest increase of in-plane capacity was observed in slender walls. For slender walls, the in-plane load capacity increased in approximately 13 to 19 times, whereas for the squat walls, it increased approximately 8 times, which proves the great contribution of the reinforcement material.

For fulfilling the equations and principles established in the ACI 440.7R-10 document, it is important that the anchoring of the wall to its foundation complies with its monolithic geometry and load transfer function. The test results demonstrated that the anchoring system used was effective. This anchorage system can provide an effective load path for masonry walls subjected to in-plane loads. The paired work of the CFRP reinforcement and the steel bars anchored to the foundation, provided an effective system to transfer and resist forces of in-plane loads.

For slender and squat walls, the 'G' layout allowed the walls to resist higher in-plane loads. Although the 'D' layout had 50% less fiber reinforcement, the 'G' layout included vertical CFRP strips at the wall ends, which can control more efficiently the horizontal flexural cracks occurring at those regions. Contrarily, in walls strengthened with the 'D' layout, the flexural cracks can travel a longer distance until reaching the first diagonal strip, which results in wider and longer cracks at the wall ends with no CFRP strips. The contribution of the horizontal CFRP strips was negligible, since all the walls primarily exhibited a flexural behavior.

The walls with the "G" layout showed less degradation of the lateral stiffness than those with the "D" layout, which proves that diagonal reinforcement layout is not recommended in walls with a high slenderness ratio, where flexural failures prevail. Referential R factors obtained for the slender and squat walls are approximately 3,6 and 2,8, respectively, indicating a substantial increase of R when compared to URM shear walls. It is important to clarify that these values are referential and should not be considered as definite values. In fact, more tests are required in order to calculate with certainty this value.

The walls did not have axial load and resistance contribution by the unreinforced masonry was very low. Therefore, flexural behavior was the most representative, and more predominant in slender walls. Although a shear failure was

desired for squat walls – as intended in some designs, it was not possible to obtain it in the developed tests.

Regarding displacements, the walls showed an elastic behavior up to a drift of approximately 0,5%. From that point, they present an inelastic behavior until they reach a maximum displacement of a drift of approximately 2,0%.

## Acknowledgements

The authors would like to acknowledge the support of the Escuela Colombiana de Ingeniería Julio Garavito for financing this project and of their staff in the Structures and Materials Laboratory, for the construction and subsequent testing of each wall; as well as the ACI committee 440 member Gustavo Tumialán and the companies Sika Colombia S.A and Ladrillera Prisma S.A., who were sponsors of this research.

## References

- ACI, Committee 440. (2010). *440.7R-10: Guide for the design and Construction of externally bonded fiber-reinforced polymer systems for strengthening unreinforced masonry structures*. (7 ed). Farmington Hills: American Concrete Institute.
- Arifuzzaman, S. & Saatcioglu, M. (2012). Seismic retrofit of load bearing masonry walls by FRP sheets and anchors. Paper presented at the Proceedings of the *15th World Conference on Earthquake Engineering*. Lisbon, Portuguese Earthquake Engineering Community. Retrieved from [http://www.iitk.ac.in/nicee/wcee/article/WCEE2012\\_4501.pdf](http://www.iitk.ac.in/nicee/wcee/article/WCEE2012_4501.pdf)
- ASCE 7-16. (2017). *Minimum design loads and associated criteria for buildings and other structures*. Reston, VA: American Society of Civil Engineers
- ASCE 41-13. (2014). *Seismic evaluation and retrofit of existing buildings*. Reston, VA: American Society of Civil Engineers
- Capozzuca, R. (2011). Experimental analysis of historic masonry walls reinforced by CFRP under in-plane cyclic loading. *Composite Structures* 94(1), 277-289. DOI: <https://doi.org/10.1016/j.compstruct.2011.06.007>
- Elgawady, M., Lestuzzi, P., & Bardoux, M. (2006). Aseismic retrofitting of unreinforced masonry walls using FRP. *Composites Part B: Engineering*, 37(2-3), 148-162. DOI: <https://doi.org/10.1016/j.compositesb.2005.06.003>
- FEMA 461. (2007). *Interim Testing Protocols for Determining the Seismic Performance Characteristics of Structural and Non structural Components*. Washington, D.C.: Federal Emergency Management Agency. Retrieved from <https://www.atcouncil.org/pdfs/FEMA461.pdf>
- FOPAE - Fondo de Prevención y Atención de Emergencias. (2010). *Visita técnica comisión de dirección de prevención y atención de emergencias - FOPAE - San Pedro de la Paz - Concepción - Chile. Informe técnico*. Bogotá D.C.: Alcaldía Mayor de Bogotá. Retrieved from <https://docplayer.es/4541826-Visita-tecnica-comision-de-direccion-de-prevencion-y-atencion-de-emergencias-fopae-san-pedro-de-la-paz-concepcion-chile-informe-tecnico.html>

- Gabor, A, Bennani, A, Jacquelin, E, & Lebon, F. (2006). Modelling approaches of the in-plane shear behaviour of unreinforced and FRP strengthened masonry panels. *Composite Structures*, 74 (3), pp. 277-288. DOI: <https://doi.org/10.1016/j.compstruct.2005.04.012>
- Galati, N., Tumialán, G., & Nanni, A. (2006). Strengthening with FRP bars of URM walls subject to out-of-plane loads. *Construction and Building Materials*, 20(1-2), 101-110. DOI: <https://doi.org/10.1016/j.conbuildmat.2005.06.047>
- Ingeominas. (1986). *El sismo de Popayán de marzo 31 de 1983*. Bogotá D.C.: Instituto Nacional de Investigaciones Geológico – Mineras.
- Ingeominas. (1999). *Terremoto del Quindío: Enero 25 de 1999. Informe Técnico Preliminar No. 2 Armenia – Quindío*. Bogotá D.C.: Instituto Nacional de Investigaciones Geológico – Mineras.
- Kalali, A., & Kabir, M. (2012). Experimental response of double-wythe masonry panels strengthened with glass fiber reinforced polymers subjected to diagonal compression tests. *Engineering Structures*, 39, 24-37. DOI: <https://doi.org/10.1016/j.engstruct.2012.01.018>
- Klingner, R. (2006). Behavior of masonry in the Northridge (US) and Tecomán - Colima (Mexico) earthquakes: Lessons learned, and changes in US design. *Construction and Building Materials*, 20(4), 209-219. DOI: <https://doi.org/10.1016/j.conbuildmat.2005.08.024>
- López, H. (2012). *Comportamiento de muros diafragma en mampostería de concreto reforzados con tejidos de FRP*. (M.Sc. thesis, Escuela Colombiana de Ingeniería). Retrieved from: <https://repositorio.escolaiing.edu.co/handle/001/211>
- Lignola, G., Prota, A., Manfredi, G. (2012). Numerical investigation on the influence of FRP retrofit layout and geometry on the in-plane behaviour of masonry walls. *Journal of Composites for Construction*, 16 (6), pp. 712-723. DOI: [https://doi.org/10.1061/\(ASCE\)CC.1943-5614.0000297](https://doi.org/10.1061/(ASCE)CC.1943-5614.0000297)
- Luccioni, B., & Rougier, V. (2011). In-plane retrofitting of masonry panels with fiber reinforced composite materials. *Construction and Building Materials*, 25(4), 1772-1788. DOI: <https://doi.org/10.1016/j.conbuildmat.2010.11.088>
- Lunn, D., Maeda, S., Rizkalla, S., & Ueda, T. (2013). Anchorage systems for FRP strengthening of infill masonry structures. *International Journal of Sustainable Materials and Structural Systems*, 1(2), 142-160. DOI: <https://doi.org/10.1504/IJSMSS.2013.056469>
- AIS. (2010). *Reglamento colombiano de construcción sismo resistente NSR-10* (Vol. 1 y Vol.2). Bogotá D.C.: Asociación de Ingeniería Sísmica.
- Mosallam, A., & Banerjee, S. (2011). Enhancement in in-plane shear capacity of unreinforced masonry (URM) walls strengthened with fiber reinforced polymer composites. *Composites Part B: Engineering*, 42(6), 1657-1670. DOI: <https://doi.org/10.1016/j.compositesb.2011.03.015>
- Paulay T., & Priestley M.J. (1992). *Seismic design of reinforced concrete and masonry buildings*. New York: Wiley.
- Rahman, A., & Ueda, T. (2016). In-plane shear performance of masonry walls after strengthening by two different FRPs. *ASCE Journal of Composites for Construction*, 20(5), 1-14. DOI: [https://doi.org/10.1061/\(ASCE\)CC.1943-5614.0000661](https://doi.org/10.1061/(ASCE)CC.1943-5614.0000661)
- Santa María, H., & Alcaino, P. (2011). Repair of in-plane shear damaged masonry walls with external FRP. *Construction and Building Materials*, 25(3), 1172-1180. DOI: <https://doi.org/10.1016/j.conbuildmat.2010.09.030>
- Triantafyllou, T., Papanicolaou, C., & Lekka, M. (2011). Externally bonded grids as strengthening and seismic retrofitting materials of masonry panels. *Construction and Building Materials*, 25(2), 504-514. DOI: <https://doi.org/10.1016/j.conbuildmat.2010.07.018>
- Tumialan, G., Vatovec, M., & Kelley, P. (2009). FRP Composites for Masonry Retrofitting: Review of Engineering Issues, Limitations and Practical Applications. *Structure magazine* (May), 12-14. Retrieved from <https://www.structuremag.org/wp-content/uploads/2014/08/C-BuildingBlocks-Tumialan-May091.pdf>
- Valluzzi, M., Tinazzi, D., & Modena, C. (2002). Shear behavior of masonry panels strengthened by FRP laminates. *Construction and Building Materials*, 16(7), 409 – 416. DOI: [https://doi.org/10.1016/S0950-0618\(02\)00043-0](https://doi.org/10.1016/S0950-0618(02)00043-0)
- Vega, C. (2015). *Comportamiento dinámico de muros de mampostería no estructural reforzados mediante polímeros reforzados con fibra de carbono, CFRP*. (M.Sc. thesis, Escuela Colombiana de Ingeniería Julio Garavito). Retrieved from <https://repositorio.escolaiing.edu.co/handle/001/211>